Journal of Materials Chemistry A

ROYAL SOCIETY OF CHEMISTRY

COMMUNICATION

View Article Online
View Journal

Cite this: DOI: 10.1039/d3ta04797k

Received 10th August 2023
Accepted 20th October 2023

DOI: 10.1039/d3ta04797k

rsc.li/materials-a

Microporous organic nanoparticles bearing tri-Zn macrocycles: heterogeneous catalysts for the conversion of biomass-derived furan esters to polymer platforms†

June Young Jang, Gang Min Lee, Jong Doo Lee and Seung Uk Son *

Biomass conversion to polymer platforms is presently a crucial issue that requires efficient catalysts. This work suggests a microporous organic polymer (MOP)-based multimetallic heterogeneous Lewis acid catalyst for the synthesis of biomass-derived polymer platforms. MOP nanoparticles bearing tri-Zn macrocycles (MOPN-TZnM) were prepared by the Sonogashira–Hagihara coupling of a predesigned building block bearing tri-Zn macrocyclic moieties with tetra(4-ethynylphenyl)methane. The MOPN-TZnM showed excellent catalytic performance in the transesterification of biomass-derived dimethyl furan-2,5-dicarboxylate with diols to furan-based diols that can be utilized as polymer platforms of polyurethanes.

Considering the severity of climate change as a critical threat to our society, it is imperative to implement regulations on the emission of carbon dioxide.[1] In view of this, strict carbon management is required in industrial production.[1] Consequently, the utilization of petroleum as a resource for material production will be limited in the future.[2] Despite petroleum-based plastics having undoubtedly facilitated a convenient lifestyle, exploring alternative resources for their production has become essential.[3]

Despite the challenges posed by climate change, carbon dioxide can be considered as a carbon source for material production.[4] However, direct capture and chemical conversion of carbon dioxide to polymer platforms entail high costs and energy.[5] Instead, carbon dioxide can be naturally fixed to chemicals, called biomass, through a process of photosynthesis. Biomass refers to organic materials derived from living or recently living organisms, such as plant matter, agricultural residues, or wood, and can be used as a renewable resource for various applications, including polymer production.[6]

Department of Chemistry, Sungkyunkwan University, Suwon 16419, Korea. E-mail: sson@skku.edu

† Electronic supplementary information (ESI) available: Experimental procedures, X-ray structure of TZnM, characterization data of MOPN-TZnM and furan-based diols. CCDC 2286971–2286972. For ESI and crystallographic data in CIF or other electronic format see DOI: https://doi.org/10.1039/d3ta04797k

Biomass primarily consists of lignocellulosic materials, comprising lignin, cellulose, and hemicellulose.[7] While lignin has been utilized as an aromatic chemical resource, the chemical conversion and utilization of cellulose and hemicellulose have captured significant attention from scientists.[8] Fig. 1 illustrates an example of the chemical modification of biomass into polymer platforms.

First, through the hydrolysis of cellulose in biomass, glucose can be produced. Subsequent isomerization of glucose and abstraction of water lead to the formation of 5-hydroxymethylfurfural (HMF).[9] Utilizing HMF as a foundational compound, various chemicals can be synthesized, collectively referred to as furanics.[10] For example, the oxidation of HMF leads to the formation of 2,5-furan dicarboxylic acid (FDCA).[10,11] FDCA serves as a monomer for the synthesis of polymers such as polyethylene furan-2,5-dicarboxylate,[12] an eco-friendly alternative to polyethylene terephthalate.

On the other hand, the chemical conversion of HMF to furan-based diols can expand the range of available polymer platforms. By reacting diols with diisocyanates, polyurethanes can be synthesized, offering versatile polymers for coating, elastomers, foams, *etc.*[10,13]

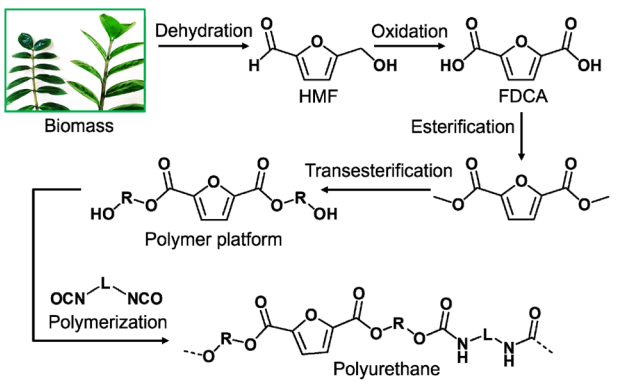

Fig. 1 Biomass conversion to furan-based polymer platforms and synthesis of polyurethanes.

The transesterification of furan esters, derived from FDCA, with diols represents an efficient method for producing furan diols.[14] However, the isolation of furan diols prepared by the transesterification of furan esters with diols is relatively rare, due to self-condensation to polyesters.[15] Lewis acid catalysts accelerate the process of transesterification.[16] While various transition metals have been employed as Lewis acid catalysts, zinc stands out due to its relatively low toxicity and cost-effectiveness.[17] Moreover, recently, multi-metallic macrocyclic complexes have emerged as promising Lewis acid catalysts.[18]

Recently, microporous organic polymers (MOPs) have been prepared through the coupling of building blocks.[19] Due to their chemical stability and porosity, MOPs can be utilized as efficient catalytic platforms.[20] In this regard, various heterogeneous catalysts bearing metal complexes have been developed to address environmental issues.[21] However, MOP-based multi-metallic heterogeneous catalysts have been rarely explored.[21]

In this work, we report the preparation of a tri-Zn macrocyclic building block (TZnM), the synthesis of MOP nanoparticles bearing TZnM (MOPN-TZnM), and their catalytic performance in the transesterification of furan esters to form furan-based diols.

Fig. 2 shows a synthetic scheme of TZnM. First, through the Duff reaction of 4-bromophenol in the presence of hexamethylenetetramine and trifluoroacetic acid,[22] 2,6-diformyl-4-bromophenol was prepared.[23] Successive reaction with *trans*-1,2-diaminocyclohexane produced an imine-based tribromo-macrocyclic compound.[24] Nuclear magnetic resonance spectroscopy (NMR) supported the formation of imine bonds with ^{1}H NMR peaks at 8.58 and 8.18 ppm (Fig. S1 in the ESI†). The imine bonds in the tribromo-macrocyclic compound were reduced to amines through a reaction with $NaBH_4$ to form a macrocyclic compound bearing amine moieties (denoted as M) (Fig. S1, S2 and Tables S1, S2 in the ESI†).[25] While the ^{1}H peaks of imine moieties completely disappeared in the ^{1}H spectrum of M, the ^{1}H peaks of methylene moieties neighboring to amines were observed at 3.82 and 3.68 ppm. Finally, zincs were introduced into M to form the target building block, TZnM, which was fully characterized by NMR and high resolution mass spectroscopy (Experimental section in the ESI†). To investigate a chemical structure of TZnM, single crystal X-ray diffraction analysis was conducted (Fig. 2, S1, S2 and Tables S1, S2 in the ESI,† CCDC# 2286971–2286972). According to the X-ray crystal structure, three zincs were coordinated to a macrocyclic ligand, M. One acetate was coordinated to zincs in the macrocyclic ligand and perchlorates existed as free counter anions. Considering labile acetate and non-coordinating perchlorates, the zincs in the M are expected to act as Lewis acidic sites.[26]

Using the TZnM as a building block, MOPN-TZnM nanoparticles were prepared by the Sonogashira–Hagihara coupling with tetra(4-ethynylphenyl)methane (Fig. 3a).

According to scanning (SEM) and transmission electron microscopy (TEM), MOPN-TZnM showed a nanoparticulate morphology with an average diameter of 245 ± 9 nm (Fig. 3b–d and S3 in the ESI†). Energy disperse X-ray spectroscopy (EDS)-based elemental mapping images showed homogeneous distribution of Zn components over MOPN-TZnM (Fig. 3e).

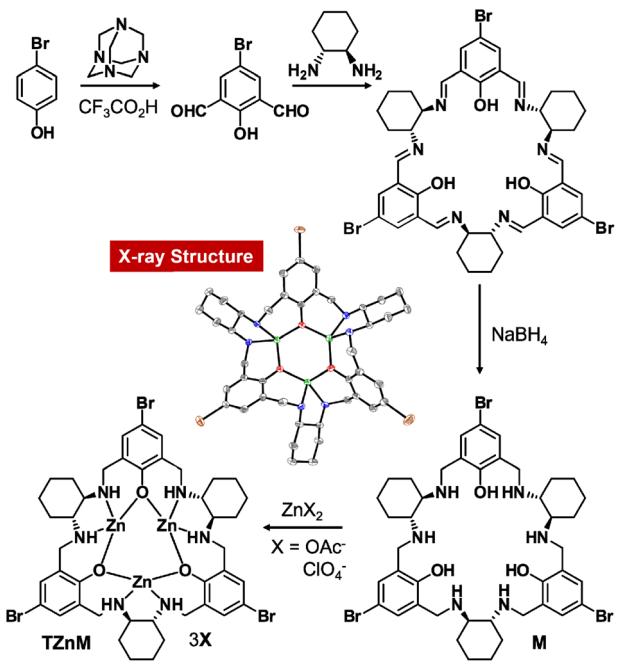

Fig. 2 Synthesis of a building block bearing tri-Zn macrocyclic complexes (TZnM) and its single crystal X-ray structure.

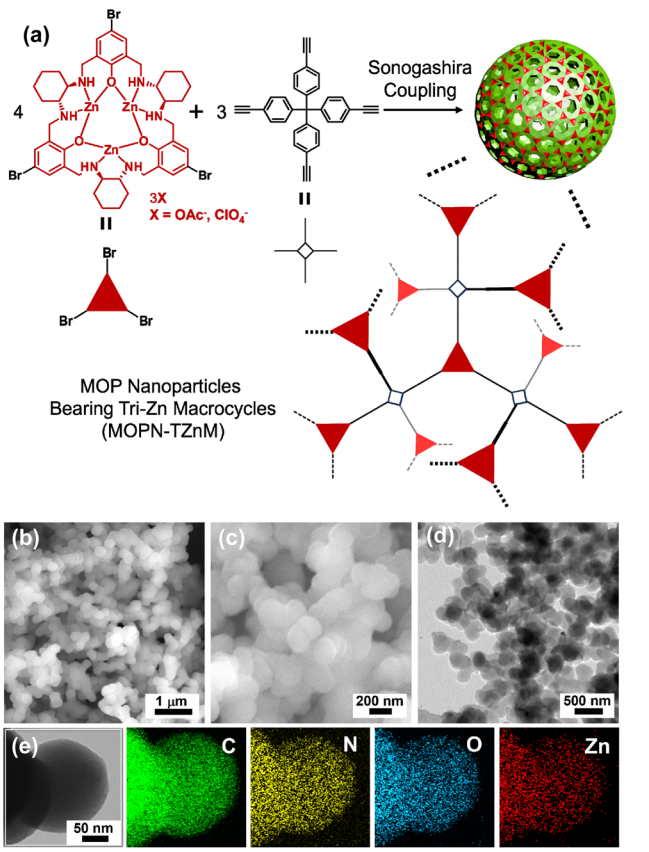

Fig. 3 (a) Synthetic scheme, (b) and (c) SEM images, (d) TEM image, and (e) EDS-elemental mapping images of MOPN-TZnM.

The surface area and porosity of MOPN-TZnM were characterized by the analysis of N_2 adsorption–desorption isotherm curves based on the Brunauer–Emmett–Teller (BET) theory, showing a high surface area of 627 $m^2\ g^{-1}$ (Fig. 4a). The pore size distribution analysis based on non-local density function theory (NLDFT) showed a microporous feature (pore sizes less than 2 nm) (inset of Fig. 4a) with a micropore volume of 0.24 $cm^3\ g^{-1}$.

Chemical structures of M, TZnM, and MOPN-TZnM were investigated by infrared (IR) absorption spectroscopy (Fig. 4b). While the C=N vibration of a precursor compound of M was observed at 1629 cm^{-1}, the IR spectrum of M showed the C–N vibration at 1227 cm^{-1} with disappearance of the C=N vibration peak at 1629 cm^{-1}, indicating that the reduction of imine to amine was completed.[27] In addition, the aliphatic C–H vibrations of M were observed at 2933, 2863, and 1453 cm^{-1}, in addition to the C–O vibration at 1107 cm^{-1}. After the coordination of Zn to M, the IR spectrum of TZnM retained the major vibration peaks of M with appearance of a vibration peak at 1114 cm^{-1}, corresponding to free perchlorate anions.[28] In the IR spectrum of MOPN-TZnM, while the main vibration peaks of TZnM were retained at 2993, 1463, 1227, and 1114 cm^{-1}, new vibration peaks were observed at 1607, 1502, and 825 cm^{-1}, corresponding to aromatic C=C and C–H vibrations originating from the tetra(4-ethynylphenyl)methane building block.[29]

A solid state ^{13}C nuclear magnetic resonance (NMR) spectrum of MOPN-TZnM showed aromatic carbon peaks at 121, 130, and 146 ppm, an sp^3 carbon peak at 64 ppm, and alkyne peaks at 85 ppm, which originated from the tetra(4-ethynylphenyl)methane building block (Fig. 4c).[30] In addition, the ^{13}C NMR spectrum of MOPN-TZnM showed aliphatic carbon peaks at 24, 29, and 57 ppm, originating from the cyclohexyl rings of M.[31] The IR and solid state ^{13}C NMR spectroscopy confirmed that the MOPN-TZnM was formed through the coupling of two building blocks.

Chemical surroundings of M, TZnM, and MOPN-TZnM were further investigated by X-ray photoelectron spectroscopy (XPS) (Fig. 5a–c). The Zn $2p_{1/2}$ and $2p_{3/2}$ orbital peaks of TZnM were observed at 1045.0 and 1021.9 eV, respectively (Fig. 5a).[32] The Zn 2p orbital peaks were retained in the XPS spectrum of MOPN-TZnM. While the locations of O 1s orbital peaks (532.0–532.2 eV) of M, TZnM, and MOPN-TZnM were not significantly different (Fig. 5b), that of the N 1s orbital peak of M was clearly distinguished from those of TZnM and MOPN-TZnM. The N 1s orbital peaks of M appeared at 398.8 and 401.1 eV, corresponding to the neutral amine species and cationic ammonium salt formed through proton transfer from hydroxyl to amine (Fig. 5c).[33] In comparison, the N 1s orbital peaks of TZnM and MOPN-TZnM were observed at 399.5 eV, indicating that the tri-Zn macrocyclic species was retained in the MOPN-TZnM.[32] According to thermogravimetric analysis (TGA), the MOPN-TZnM was thermally stable up to 325 °C (Fig. 5d). Powder X-ray diffraction (PXRD) studies showed that MOPN-TZnM is amorphous, matching with the conventional feature of MOP materials prepared by the Sonogahsira–Haghihara coupling of organic building blocks (Fig. S4 in the ESI†).[34] The Zn content in MOPN-TZnM was analyzed to be 0.83 mmol g^{-1} by inductively coupled plasma-atomic emission spectroscopy (ICP-AES).

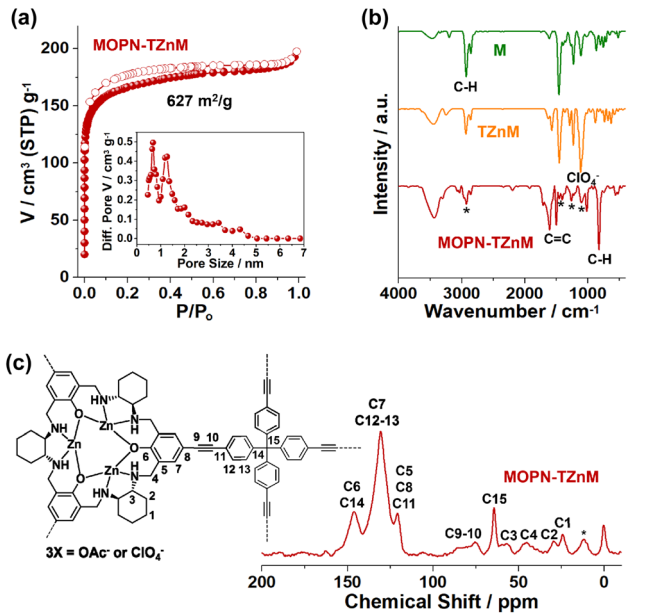

Fig. 4 (a) N_2 adsorption–desorption isotherm curves obtained at 77 K (inset: a pore size distribution diagram based on the NLDFT method) of MOPN-TZnM, (b) IR spectra of M, TZnM, and MOPN-TZnM (asterisks in the IR spectrum of MOPN-TZnM indicate the chemical moieties originating from TZnM), and (c) a solid state ^{13}C NMR spectrum of MOPN-TZnM (the peak indicated by an asterisk corresponds to grease).

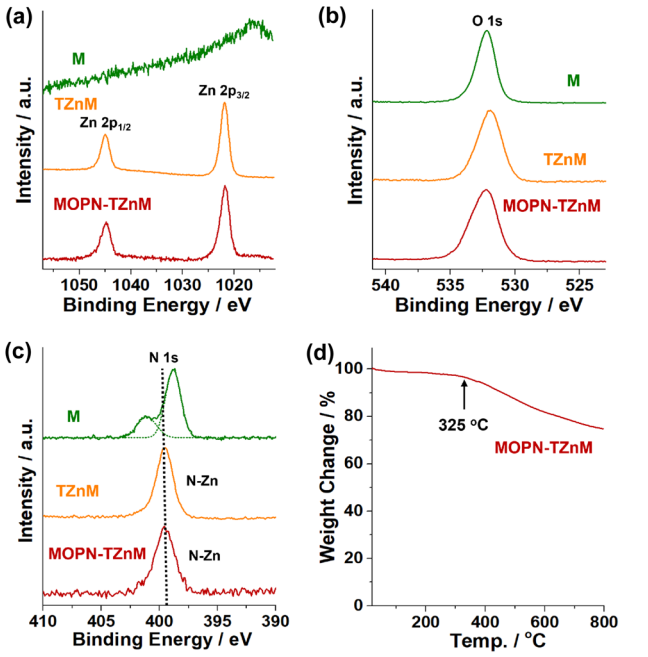

Fig. 5 (a) XPS Zn 2p orbital spectra, (b) XPS O 1s orbital spectra, and (c) XPS N 1s orbital spectra of M, TZnM, and MOPN-TZnM. (d) A TGA curve of MOPN-TZnM.

Next, considering the high surface area, porosity, and potential Lewis acid feature of MOPN-TZnM, we studied its catalytic performance for the transesterification of furan ester (dimethyl furan-2,5-dicarboxylate, FDCA-DM) with various diols to furan-based diols.[15] Table 1 summarizes the results.

First, the reaction conditions for the transesterification of FDCA-DM with 2,2′-oxydiethanol (**D1**), catalyzed by MOPN-TZnM, were optimized. When MOPN-TZnM with 2.0 mol% Zn was used, the conversion yields of FDCA-DM with **D1** to the corresponding furan diol gradually increased from 11% to 59, 80, 94, and 99% (an isolated yield of 92%) at 150 °C after 0.5, 1.5, 3, 6, and 9 h, respectively (entries 1–5 in Table 1). When the amount of MOPN-TZnM was reduced to 1.5 mol% Zn or no catalyst was used, the conversion yields of FDCA-DM to a furan diol at 150 °C after 9 h were dropped to 91 and 13%, respectively (entries 6–7 in Table 1). When the reaction temperature decreased from 150 °C to 130 °C, the conversion yields of FDCA-DM after 9 h decreased from 99% to 74% (entry 8 in Table 1). The MOPN-TZnM with 2.0 mol% Zn, 150 °C, and 9 h were determined as optimized reaction conditions.

Table 1 Catalytic transesterification of dimethyl furan-2,5-dicarboxylate (FDCA-DM) with various diols by MOPN-TZnM[a]

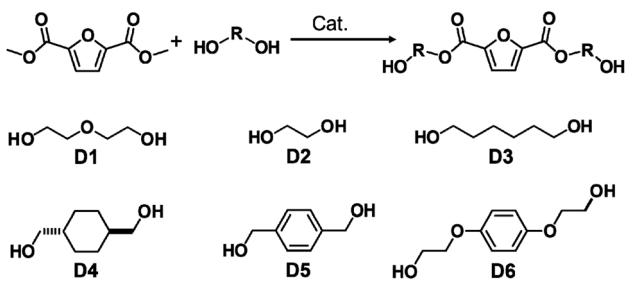

Entry	Cat (mol%)	Diols	Time (h)	Yield[b] (%)
1	2	**D1**	0.5	11
2	2	**D1**	1.5	59
3	2	**D1**	3	80
4	2	**D1**	6	94
5	2	**D1**	9	99(92)
6	1.5	**D1**	9	91
7	0	**D1**	9	13
8[c]	2	**D1**	9	74
9	2	**D2**	9	98(90)
10	2	**D3**	9	84
11	2	**D3**	18	99(93)
12	2	**D4**	9	59
13	2	**D4**	18	77
14	2	**D4**	36	96(90)
15	2	**D5**	9	80
16	2	**D5**	18	94(87)
17	2	**D6**	9	30
18	2	**D6**	18	64
19	2	**D6**	36	91(87)
20[d]	2	**D1**	9	99
21[e]	2	**D1**	9	97
22[f]	2	**D1**	9	97
23[g]	2	**D1**	9	96

[a] Reaction conditions: dimethyl furan-2,5-dicarboxylate (FDCA-DM, 0.50 mmol), diols (2.0 mmol), MOPN-TZnM (0.83 mmol Zn per g based on the ICP-AES analysis, 12 mg, 2.0 mol% Zn for FDCA-DM), toluene (1 mL), 150 °C. [b] Conversion yields of FDCA-DM (isolated yields of furan diols were given in parentheses). [c] Reaction temperature of 130 °C. [d] The catalyst recovered from entry 5 was used. [e] The catalyst recovered from entry 20 was used. [f] The catalyst recovered from entry 21 was used. [g] The catalyst recovered from entry 22 was used.

Various diols (**D2–D6**, entries 9–19 in Table 1) were tested for the transesterification of FDCA-DM to furan diols under optimized reaction conditions. When ethane-1,2-diol (**D2**) was used for the transesterification of FDCA-DM, a good conversion yield of 98% (an isolated yield of 90%) was observed (entry 9 in Table 1) at 150 °C after 9 h. In the cases of diols with a relatively longer chain or a bulkier bridging group, longer reaction times were required (entries 10–14 in Table 1). When hexane-1,6-diol (**D3**) was used for the transesterification of FDCA-DM, the reactions showed conversion yields of 84 and 99% (an isolated yield of 93%) at 150 °C after 9 and 18 h, respectively (entries 10–11 in Table 1). *Trans*-1,4-di(hydroxymethyl)cyclohexane (**D4**) required further longer reaction times for the transesterification of FDCA-DM, showing conversion yields of 59, 77, and 96% (an isolated yield of 90%) at 150 °C after 9, 18, and 36 h (entries 12–14 in Table 1).

Diols with aromatic bridging groups were studied as substrates for the transesterification of FDCA-DM (entries 15–19 in Table 1). When 1,4-phenylenedimethanol (**D5**) was used, conversion yields of 80 and 94% (an isolated yield of 87%) were observed after 9 and 18 h, respectively (entries 15–16 in Table 1). Finally, when 2,2′-(1,4-phenylenebis(oxy))diethanol (**D6**) was used, conversion yields of 30, 64, and 91% (an isolated yield of 87%) were obtained after 9, 18 and 36 h, respectively (entries 17–19 in Table 1). In addition to the diols listed in Table 1, we also tested three additional diols for the transesterification of FDCA-DM. However, when anthracene-9,10-diyldimethanol was used, the transesterification did not proceed, due to its poor solubility. Additionally, both (2-methoxy-1,4-phenylene) dimethanol and (2-nitro-1,4-phenylene)dimethanol proved ineffective for the transesterification of FDCA-DM, due to the steric hindrance caused by the *ortho* functional groups.

When the Zn metals in MOPN-TZnM were etched using HCl solution, the resultant MOPN-M did not exhibit catalytic activity in the transesterification of FDCA-DM with **D1**. This suggests that the Zn metals in MOPN-TZnM functioned as Lewis acid catalysts (refer to the mechanism in Fig. S5 in the ESI†).[35]

The recyclability of MOPN-TZnM was studied (entries 5 and 20–23 in Table 1 and Fig. 6). After transesterification of FDCA-DM with **D1** for 9 h, the catalyst was recovered through centrifugation, washed, dried, and reused for the next reaction. As shown in Fig. 6a, the MOPN-TZnM retained the catalytic performance for five successive runs with conversion yields of 96–99%. According to TEM analysis, the recovered catalyst retrieved after five successive runs showed the retention of the original morphology (Fig. 6b). In the IR and NMR studies, while the original chemical structure of MOPN-TZnM was retained, an additional vibration peak appeared at 1119 cm^{-1}, corresponding to the C–O vibration, due to the diols or furan diols entrapped in MOP networks (Fig. 6c and S6 in the ESI†). The original Zn 2p orbitals at 1045.0 and 1021.9 eV and the N 1s

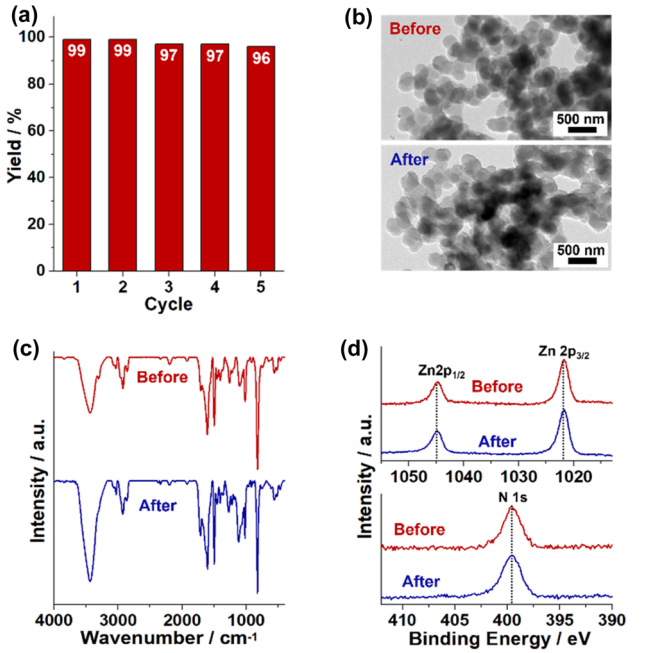

Fig. 6 (a) Recyclability tests of the MOPN-TZnM catalyst for the transesterification of FDCA-DM with 2,2′-oxydiethanol (**D1**) to furan diol, (b) TEM images, (c) IR spectra, and (d) XPS spectra of the Zn 2p orbitals and N 1s orbital of MOPN-TZnM before and after five successive runs.

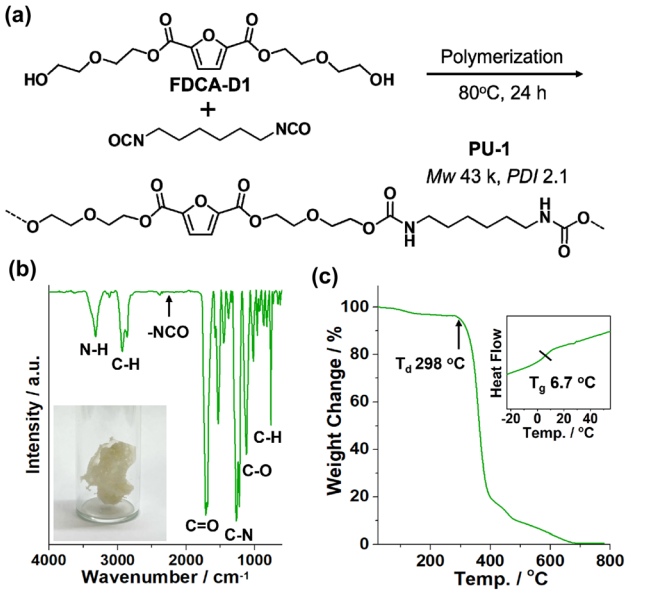

Fig. 7 Demonstration of the polyurethane synthesis using the furan diol prepared in this study: (a) a reaction scheme for the synthesis of polyurethane (PU-1) using the furan diol (FDCA-**D1**) prepared by transesterification of FDCA-DM with **D1** and 1,6-diisocyanatohexane. (b) IR spectrum (inset: a photography of PU-1) and (c) a TGA curve (inset: a DSC curve) of PU-1.

orbital peak at 399.5 eV were retained in the XPS spectrum of MOPN-TZnM recovered after five runs, indicating the maintenance of Zn–N species (Fig. 6d).

Recently, Lewis acid catalytic systems for the transesterification of furan esters with diols have been reported in the literature.[15] However, homogeneous catalysts have been used and the resultant products were furan-based polyesters that were formed through successive polymeric condensation between furan-based diols.[15] In comparison, the MOPN-TZnM-based heterogeneous catalytic system of this work provides various furan-based diols that can be utilized for the synthesis of polyurethanes (Fig. S7 in the ESI†).

Using a furan-based diol (FDCA-**D1**) prepared by the catalytic transesterification of FDCA-DM with **D1**, we demonstrated the synthesis of polyurethane (Fig. 7 and S8 in the ESI†).[36] An ivory-colored polyurethane (PU-1) was formed through a direct reaction of the furan diol with 1,6-diisocyanatohexane at 80 °C for 24 h (Fig. 7a and inset in Fig. 7b). PU-1 was retrieved from a reaction mixture through recrystallization in methanol solution. According to gel permeation chromatography (GPC) analysis, the molecular weight and polydispersity index (PDI) of PU-1 were measured to be and 43 000 (M_w) and 2.1, respectively. In IR analysis, while the vibration peak of isocyanate groups disappeared at 2268 cm^{-1}, C–O, C–N, C═O, and N–H peaks were observed at 1100, 1245, 1765, and 3318 cm^{-1}, respectively, indicating formation of urethane bonds in PU-1.[36]

According to TGA and differential scanning calorimeter (DSC) analysis, PU-1 has a decomposition temperature (T_d) of 298 °C and a glass transition temperature (T_g) of 6.7 °C (Fig. 7c).

In addition, we found that PU-1 can be used as a coating material for solid supports. Extensive application studies are ongoing for PUs that can be prepared using the furan diols in this study.

In conclusion, a novel building block containing a tri-Zn macrocycle was successfully synthesized and its structure was characterized using single crystal X-ray diffraction analysis, aiming to create a MOP-based heterogeneous Lewis acid catalyst. By conducting the Sonogashira–Hagihara coupling of the building block with tetra(4-ethynylphenyl)methane, MOPN-TZnM was synthesized, exhibiting a high surface area of 627 $m^2 g^{-1}$ and microporosity. The MOPN-TZnM, with 2.0 mol% Zn showed excellent catalytic performance in the transesterification of biomass-derived FDCA-DM with diols to produce furan-based diols. The catalyst also demonstrated excellent recyclability over five successive runs. Furthermore, by utilizing various diols, diverse furan-based diols could be prepared, offering potential applications in polyurethane synthesis. Considering the results, we propose that MOPN-TZnM can serve as an effective Lewis acid catalyst for the various conversions of biomass and carbon dioxide to valuable chemicals. Furthermore, the Zn metals in MOPN-TZnM can be replaced with new metals through Zn etching followed by the incorporation of new metals (Fig. S9 in the ESI†), allowing for the development of novel catalysts.

Author contributions

S. U. Son: conceptualization, supervision, writing original draft, and review & editing. J. Y. Jang, K. M. Lee, and J. D. Lee: investigation and formal analysis.

Conflicts of interest

There are no conflicts to declare.

Acknowledgements

This work was supported by the Carbon Upcycling Project for Platform Chemicals (No. 2022M3J3A1046019) and by the National Research Foundation of Korea (NRF) grants (No. RS-2023-00208797) funded by the Korea government (MSIT).

Notes and references

1 (*a*) Z. Liu, Z. Deng, S. Davis and P. Ciais, *Nat. Rev. Earth Environ.*, 2023, **4**, 205–206; (*b*) S. Solomon, G.-K. Plattner, R. Knutti and P. Friedlingstein, *Proc. Natl. Acad. Sci. U. S. A.*, 2009, **106**, 1704–1709.

2 S. Bathrinath, N. Abuthakir, K. Koppiahraj, S. Saravanasankar, T. Rajpradeesh and R. Manikandan, *Mater. Today: Proc.*, 2021, **46**, 7798–7802.

3 R. Mori, *RSC Sustainability*, 2023, **1**, 179–212.

4 (*a*) J. Artz, T. E. Müller and K. Thenert, *Chem. Rev.*, 2018, **118**, 434–504; (*b*) S. C. Peter, *ACS Energy Lett.*, 2018, **3**, 1557–1561.

5 (*a*) C. Kim, C.-J. Yoo, H.-S. Oh, B. K. Min and U. Lee, *J. CO_2 Util.*, 2022, **65**, 102239; (*b*) H.-J. Ho, A. Iizuka and E. Shibata, *Ind. Eng. Chem. Res.*, 2019, **58**, 8941–8954; (*c*) E. S. Sanz-Pérez, C. R. Murdock, S. A. Didas and C. W. Jones, *Chem. Rev.*, 2016, **116**, 11840–11876.

6 (*a*) M. Schubert, G. Panzarasa and I. Burgert, *Chem. Rev.*, 2023, **123**, 1889–1924; (*b*) K. Huang, X. Peng, L. Kong, W. Wu, Y. Chen and C. T. Maravelias, *ACS Sustainable Chem. Eng.*, 2021, **9**, 14480–14487.

7 H. Zhu, W. Luo, P. N. Ciesielski, Z. Fang, J. Y. Zhu, G. Henriksson, M. E. Himmel and L. Hu, *Chem. Rev.*, 2016, **116**, 9305–9374.

8 (*a*) L. Lin, X. Han, B. Han and S. Yang, *Chem. Soc. Rev.*, 2021, **50**, 11270–11292; (*b*) B. M. Upton and A. M. Kasko, *Chem. Rev.*, 2016, **116**, 2275–2306; (*c*) M. Besson, P. Gallezot and C. Pinel, *Chem. Rev.*, 2014, **114**, 1827–1870.

9 (*a*) M. E. Zakrzewska, E. Bogel-Lukasik and R. Bogel-Lukasik, *Chem. Rev.*, 2011, **111**, 397–417; (*b*) J. B. Binder and R. T. Raines, *J. Am. Chem. Soc.*, 2009, **131**, 1979–1985.

10 (*a*) Y. Meng, S. Yang and H. Li, *ChemSusChem*, 2022, **15**, e202102581; (*b*) F. Chacón-Huete, C. Messina, B. Cigana and P. Forgione, *ChemSusChem*, 2022, **15**, e202200328; (*c*) B. R. Caes, R. E. Teixeira, K. G. Knapp and R. T. Raines, *ACS Sustainable Chem. Eng.*, 2015, **3**, 2591–2605.

11 (*a*) H. S. Jeong, S. H. Ryu, Y. Myung, S. M. Lee, H. J. Kim and S. U. Son, *ACS Appl. Nano Mater.*, 2022, **5**, 4603–4680; (*b*) S. E. Davis, L. R. Houk, E. C. Tamargo, A. K. Datye and R. J. Davis, *Cat. Today*, 2011, **160**, 55–60.

12 (*a*) X. Fei, J. Wang, J. Zhu, X. Wang and X. Liu, *ACS Sustainable Chem. Eng.*, 2020, **8**, 8471–8485; (*b*) J.-G. Rosenboom, D. K. Hohl, P. Fleckenstein, G. Storti and M. Morbidelli, *Nat. Commun.*, 2018, **9**, 2701.

13 H. Chang, E. B. Gilcher, G. W. Huber and J. A. Dumesic, *Green Chem.*, 2021, **23**, 4355–4364.

14 Z. Deng, I. Liubchak, F. B. Holness, F. Shahrokhi, A. D. Price and E. R. Gillies, *J. Polym. Sci.*, 2023, **61**, 1528–1536.

15 (*a*) A. Shen, J. Wang, X. Zhang, X. Fei, L. Fan, Y. Zhu, Y. Dong and J. Zhu, *J. Appl. Polym. Sci.*, 2022, **139**, e52469; (*b*) X. Fei, Y. Zhu, J. Wang, Z. Jia and X. Liu, *Polym. Adv. Technol.*, 2022, **33**, 2265–2275; (*c*) J. Wang, X. Liu, Z. Jia, L. Sun and J. Zhu, *Eur. Polym. J.*, 2018, **109**, 379–390; (*d*) M. Matos, A. F. Sousa and A. J. D. Silvestre, *Macromol. Chem. Phys.*, 2017, **218**, 1600492; (*e*) Z. Terzopoulou, E. Karakatsianopoulou, N. Kasmi, V. Tsanaktsis, N. Nikolaidis, M. Kostoglou, G. Z. Papageorgiou, D. A. Lambropoulou and D. N. Bikiaris, *Polym. Chem.*, 2017, **8**, 6895–6908; (*f*) S. Hong, K.-D. Min, B.-U. Nam and O. O. Park, *Green Chem.*, 2016, **18**, 5142–5150.

16 (*a*) R. Esposito, M. Melchiorre, A. Annunziata, M. E. Cucciolito and F. Ruffo, *ChemCatChem*, 2020, **12**, 5858–5879; (*b*) D. Nakatake, R. Yazaki, Y. Matsushima and T. Ohshima, *Adv. Synth. Catal.*, 2016, **358**, 2569–2574; (*c*) M. Hatano and K. Ishihara, *Chem. Commun.*, 2013, **49**, 1983–1997; (*d*) A. Pericas, A. Shafir and A. Vallribera, *Tetrahedron*, 2008, **64**, 9258–9263.

17 (*a*) W. Zhang, R. Ping, X. Lu, H. Shi, F. Liu, J. Ma and M. Liu, *Chem. Eng. J.*, 2023, **451**, 138715; (*b*) J. Wang, J. Wang, Y. Liu, T. Liu, Z. Pang, H. Cui, Y. Zhang and F. Song, *Green Chem.*, 2023, **25**, 5613–5625; (*c*) Y. Yang, J. D. Lee, Y. H. Seo, J.-H. Chae, S. Bang, Y.-J. Cheong, B. Y. Lee, I.-H. Lee, S. U. Son and H.-Y. Jang, *Dalton Trans.*, 2022, **51**, 16620–16627; (*d*) N. Haque, S. Biswas, S. Ghosh, A. H. Chowdhury, A. Khan and S. M. Islam, *ACS Appl. Nano Mater.*, 2021, **4**, 7663–7674; (*e*) Y. Xie, T.-T. Wang, R.-X. Yang, N.-Y. Huang, K. Zou and W.-Q. Deng, *ChemSusChem*, 2014, **7**, 2110–2114; (*f*) S. Klaus, M. W. Lehenmeier, E. Herdtweck, P. Deglmann, A. K. Ott and B. Rieger, *J. Am. Chem. Soc.*, 2011, **133**, 13151–13161.

18 (*a*) X. Liao, J.-H. He and Y.-T. Zhang, *Chem.–Asian J.*, 2023, **18**, e202201076; (*b*) T. M. McGuire, A. C. Deacy, A. Buchard and C. K. Williams, *J. Am. Chem. Soc.*, 2022, **144**, 18444–18449; (*c*) A. J. Plajer and C. K. Williams, *Angew. Chem., Int. Ed.*, 2021, **60**, 13372–13379; (*d*) J. Chen, X. Wu, H. Ding, N. Liu, B. Liu and L. He, *ACS Sustainable Chem. Eng.*, 2021, **9**, 16210–16219; (*e*) F. de la Cruz-Martínez, M. M. d. S. Buchaca, J. Martínez, J. Tejeda, J. Fernández-Baeza, C. Alonso-Moreno, A. M. Rodriguez, J. A. Castro-Osma and A. Lara-Sánchez, *Inorg. Chem.*, 2020, **59**, 8412–8423; (*f*) J. R. Pankhurst, S. Paul, Y. Zhu, C. K. Williams and J. B. Love, *Dalton Trans.*, 2019, **48**, 4887–4893; (*g*) J. Bai, X. Xiao, Y. Zhang, J. Chao and X. Chen, *Dalton Trans.*, 2017, **46**, 9846–9858; (*h*) C.-Y. Yu, H.-J. Chuang and B.-T. Ko, *Catal. Sci. Technol.*, 2016, **6**, 1779–1791; (*i*) X. Liu, P. Du and R. Cao, *Nat. Commun.*, 2013, **4**, 2375.

19 (*a*) K. Cho, C. W. Kang, S. H. Ryu, J. Y. Jang and S. U. Son, *J. Mater. Chem. A*, 2022, **10**, 6950–6954; (*b*) J.-S. M. Lee and A. I. Cooper, *Chem. Rev.*, 2020, **120**, 2171–2214.

20 (*a*) G. Ji, Y. Zhao and Z. Liu, *Green Chem. Eng.*, 2022, **3**, 96–110; (*b*) Y. Gu, S. U. Son, T. Li and B. Tan, *Adv. Funct. Mater.*, 2020, 2008265; (*c*) Y.-B. Zhou and Z.-P. Zhan, *Chem.–Asian J.*, 2018, **13**, 9–19; (*d*) Y. Zhang and

S. N. Riduan, *Chem. Soc. Rev.*, 2012, **41**, 2083–2094; (*e*) P. Kaur, J. T. Hupp and S. T. Nguyen, *ACS Catal.*, 2011, **1**, 819–835.

21 (*a*) J. I. Park, J. Y. Jang, Y.-J. Ko, S. M. Lee, H. J. Kim, H.-Y. Jang, K. C. Ko and S. U. Son, *Chem.–Asian J.*, 2021, **16**, 1398–1402; (*b*) K. Cho, S. M. Lee, H. J. Kim, Y.-J. Ko, E. J. Kang and S. U. Son, *Chem.–Eur. J.*, 2020, **26**, 788–794; (*c*) M. H. Kim, T. Song, U. R. Seo, J. E. Park, K. Cho, S. M. Lee, H. J. Kim, Y.-J. Ko, Y. K. Chung and S. U. Son, *J. Mater. Chem. A*, 2017, **5**, 23612–23619.

22 (*a*) J. C. Duff, *J. Chem. Soc.*, 1941, 547–550; (*b*) J. C. Duff, *J. Chem. Soc.*, 1945, 276–277; (*c*) J. C. Duff and V. J. Furness, *J. Chem. Soc.*, 1951, 1512–1515; (*d*) W. E. Smith, *J. Org. Chem.*, 1972, **37**, 3972–3973.

23 W. A. A. Arafa, M. D. Karkas, B.-L. Lee, T. Akermark, R.-Z. Liao, H.-M. Berends, J. Messinger, P. E. M. Siegbahn and B. Akermark, *Phys. Chem. Chem. Phys.*, 2014, **16**, 11950–11964.

24 M. Petryk, A. Troc, B. Cierczyk, W. Danikiewicz and M. Kwit, *Chem.–Eur. J.*, 2015, **21**, 10318–10321.

25 J. Gao, R. A. Zingaro, J. H. Reibenspies and A. E. Martell, *Org. Lett.*, 2004, **6**, 2453–2455.

26 S. R. Korupoju, N. Mangayarkarasi, P. S. Zacharias, J. Mizuthani and H. Nishihara, *Inorg. Chem.*, 2002, **41**, 4099–4101.

27 P. Ju, W. Qi, B. Guo, W. Liu, Q. Wu and Q. Su, *Catal. Lett.*, 2023, **153**, 2125–2136.

28 N. He, Y. Ni, J. Teng, H. Li, L. Yao and P. Zhao, *Spectrochim. Acta, Part A*, 2019, **221**, 117164.

29 C. W. Kang, D.-M. Lee, J. Park, S. Bang, S.-W. Kim and S. U. Son, *Angew. Chem., Int. Ed.*, 2022, **61**, e202209659.

30 S. Bang, J. Y. Jang, Y.-J. Ko, S. M. Lee, H. J. Kim and S. U. Son, *ACS Macro Lett.*, 2022, **11**, 1034–1040.

31 J. Gao and E. Martell, *Org. Biomol. Chem.*, 2003, **1**, 2795–2800.

32 C. Xie, L. Lin, L. Huang, Z. Wang, Z. Jiang, Z. Zhang and B. Han, *Nat. Commun.*, 2021, **12**, 4823.

33 M. Kehrer, J. Duchoslav, A. Hinterreiter, M. Cobet, A. Mehic, T. Stehrer and D. Stifter, *Plasma Processes Polym.*, 2019, **16**, e1800160.

34 R. S. Sprick, J.-X. Jiang, B. Bonillo, S. Ren, T. Ratvijitvech, P. Guiglion, M. A. Zwijnenburg, D. J. Adams and A. I. Copper, *J. Am. Chem. Soc.*, 2015, **137**, 3265–3270.

35 R. Esposito, M. Melchiorre, A. Annunziata, M. E. Cucciolito and F. Ruffo, *ChemCatChem*, 2020, **12**, 5858–5879.

36 (*a*) C. Oh, E. H. Choi, E. J. Choi, T. Premkumar and C. Song, *ACS Sustainable Chem. Eng.*, 2020, **8**, 4400–4406; (*b*) H. Sardon, A. Pascual, D. Mecerreyes, D. Taton, H. Cramail and J. L. Hedrick, *Macromolecules*, 2015, **48**, 3153–3465.